A Letters Journal Exploring the Frontiers of Physics

January 2010

EPL, **89** (2010) 18002
doi: 10.1209/0295-5075/89/18002

www.epljournal.org

Dynamical processes on dissortative scale-free networks

J. Menche[(a)], A. Valleriani and R. Lipowsky[(b)]

Max-Planck-Institute of Colloids and Interfaces - Science Park Golm, 14424 Potsdam, Germany, EU

received 22 October 2009; accepted in final form 8 December 2009
published online 18 January 2010

PACS 89.75.-k – Complex systems
PACS 05.50.+q – Lattice theory and statistics (Ising, Potts, etc.)
PACS 89.75.Hc – Networks and genealogical trees

Abstract – Many real-world networks exhibit scale-free degree distributions together with dissortative degree correlations. Such networks exhibit interesting structural and dynamical features, especially in the limit of maximal correlations. In the latter case, the network vertices are shown to form nested bilayers, the number of which grows with network size N but saturates for large N. This bilayer structure strongly affects the properties of dynamical processes on such networks and implies a large number of attractors that govern the long-time behavior of these processes. Surprisingly, the most complex dynamical behavior is found for intermediate rather than for large network sizes.

Introduction. – During the last decade, many complex systems have been described as networks of interacting units that evolve with time [1,2]. Biological examples include transcriptional gene networks [3], cell-cycle regulation [4], neural networks [5], and the immune system [6]. The long-time behavior of these dynamical processes is governed by their so-called attractors. In this article, we study the attractors for generic processes on networks that exhibit two widespread structural features. First, many networks have been found to have a scale-free degree distribution, *i.e.*, the probability that a randomly chosen vertex has k neighbors or degree k behaves as $P(k) \sim k^{-\gamma}$ [7,8]. Second, especially biological and technological networks often exhibit so-called dissortative mixing [9,10], *i.e.*, the tendency that high-degree vertices are preferably connected to low-degree vertices.

It turns out, however, that the possible correlation profiles of scale-free networks are restricted by the degree distribution of these networks. In this article, we introduce and study maximally dissortative networks, which exhibit particularly interesting structural and dynamical properties. We first show that their vertices form nested bilayers, the number of which grows with network size N but *saturates* for large N. We then study generic dynamical processes on these networks and find that these processes are strongly affected by the networks' bilayer structure. Indeed, the different vertex bilayers can be dynamically decoupled giving rise to complex dynamical behavior with a large number of attractors.

Dynamical systems can often be described by two-state systems. Biological examples are provided by firing and nonfiring neurons in neural networks or the regulation of genetic networks with patterns of active and inactive genes. Of particular interest are the properties of the dynamical attractors, since they correspond to relevant states of the underlying systems. For the identification and understanding of generic features, it is advantageous to study relatively simple processes. One of the simplest dynamical processes is provided by majority rule dynamics. The local updating rule corresponds to Glauber dynamics at zero temperature in Ising-spin systems [11] and has been studied in various contexts for different network topologies, see, *e.g.*, [3–6,11–18]. For scale-free networks without degree-degree correlations, majority rule dynamics was found to be governed by only two stable fixed points [15,16].

In this article, we study majority rule dynamics on dissortative scale-free networks and focus on the case of maximal dissortativity. We show that these latter networks are characterized by a huge number of attractors in contrast to the uncorrelated case. Using extensive numerical computations, we estimate the number of attractors $\mathcal{N}_{\mathrm{A}}$ as a function of network size N. We derive an upper bound on $\mathcal{N}_{\mathrm{A}}$ that attains a constant value for large N. In addition, we find that the total number of attractors attains a maximum at *intermediate* values of N. This nonmonotonic behavior in the overall dynamical

[(a)] E-mail: menche@mpikg.mpg.de
[(b)] E-mail: lipowsky@mpikg.mpg.de

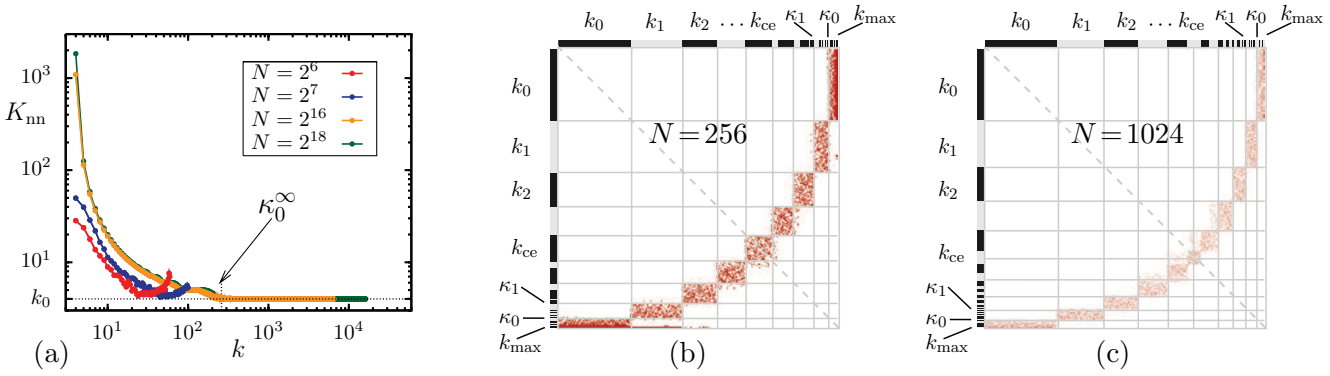

Fig. 1: Structural properties: (a) average nearest-neighbor degree $K_{\rm nn}$ as a function of degree k for different N with $\gamma = 2.5$, $k_0 = 4$, averaged over 100 networks; (b), (c) adjacency matrices $\mathbf{A}$ for two networks with $N = 256$ and $N = 1024$ vertices, both for $\gamma = 2.9$ and $k_0 = 6$. The vertices are ordered according to their degree k with $k_0 < k_1 < k_2 < \cdots < k_{\rm max}$. The bars at the left and upper boundary have a length proportional to the number of vertices with the indicated degree. Each red dot represents a nonzero matrix element $A_{ij} = 1$. Because of $A_{ji} = A_{ij}$, the diagrams are symmetric with respect to the dashed diagonal and to the central $k_{\rm ce}$-cluster with $k_{\rm ce} = k_4$ and $k_{\rm ce} = k_5$ in (b) and (c). As explained in the text, the rectangular nondiagonal clusters correspond to bilayers, in which vertices of the low degree k_n are connected to vertices with high degrees $\kappa_n < k < \kappa_n - 1$.

complexity is robust and does not depend on the structural details of the networks as described at the end of this letter.

Network structure. – The networks considered here have the scale-free degree distribution

$$P(k) = \frac{1}{\mathcal{A}} k^{-\gamma} \quad \text{for} \quad k_0 \leqslant k \leqslant k_{\rm max}, \tag{1}$$

with the normalization constant $\mathcal{A} \equiv \sum_k k^{-\gamma}$. The structural parameters of these networks are the size N, the exponent γ of the degree distribution, and the lower cut-off k_0. In our simulations, we explore the range $2 < \gamma < 3$, which is the range of most real-world networks [7,8]. We will explicitly describe our results for undirected, simple networks without multiple edges and self-connections and with the so-called natural cut-off $k_{\rm max} = \min(N-1, k_0 N^{\frac{1}{\gamma-1}})$ [19]. Several extensions will also be discussed.

The most widely used measures for dissortative correlations in networks are i) the Pearson correlation coefficient r for the degrees of the vertices at the two ends of an edge [9,10], ii) the conditional probability $P(k|k')$ that an edge emerging from a vertex with degree k' points to a vertex with degree k [20], and iii) the average degree of the nearest neighbors of a randomly picked vertex with degree k as defined by $K_{\rm nn}(k) \equiv \sum_k k P(k|k')$ [21].

The networks are constructed in two steps, starting with the well-known configuration model [22]: first, the degrees $k_1, k_2, \ldots, k_N$ are drawn from the distribution $P(k)$ in (1) and attached to the vertices as half-edges or "stubs". Then, randomly chosen pairs of such stubs are combined into full edges. The construction of simple networks without multiple edges and self-connections requires an additional intermediate check: if a randomly chosen pair of stubs leads to multiple edges or self-connections, this pair is simply discarded and a new one is drawn until all stubs are connected.

In a second step, dissortative correlations are incorporated into this network by applying a rewiring scheme as described in [23]. In each iteration of this algorithm, two edges that connect four different vertices are chosen at random. These edges are broken up again into half edges and rewired, in such a way that the two vertices with the highest and the lowest degrees are connected. For simple networks, we again discard forbidden connections. The procedure does not change the degree distribution and ultimately leads to a *maximally* dissortative network, for which r attains its minimal negative value and the average nearest-neighbor degree $K_{\rm nn}$ strongly decreases with k, see fig. 1(a).

Further analysis shows that the structure of *small* networks is dominated by the highly connected hubs. For simple networks with $N < N_1 \equiv k_0^{(\gamma-1)/(\gamma-2)}$, the vertex with maximal degree $k_{\rm max} = N - 1$ is connected to *all* other vertices in the network. This property leads to the small increase of $K_{\rm nn}(k)$ close to $k = k_{\rm max}$, see fig. 1(a) for $N = N_1 = 2^6$ and $N = 2^7$. For network size $N > N_1$, the hubs do no longer span the entire networks, but are still connected to several layers of low-degree vertices with $k_0 \leqslant k \leqslant k_A$ and

$$k_A \equiv k_0 \left[1 - \left(1 - \frac{1}{N} \right) k_0 N^{\frac{2-\gamma}{\gamma-1}} \right]^{\frac{1}{1-\gamma}}, \tag{2}$$

which behaves as $k_A \approx k_0$ for large N.

In addition to these subgraphs connected by the hubs, the vertices of dissortative scale-free networks are found to form nested bilayers, the number of which grows with N. This property can be directly visualized by the adjacency matrix $\mathbf{A}$, which has $N \times N$ entries A_{ij} with $A_{ij} = 1$ if the vertices i and j are connected and $A_{ij} = 0$, otherwise.

When the vertices are ordered according to their degree, the nonzero entries $A_{ij} = 1$ form a "necklace" of clusters that correspond to groups of vertices with the same

degree, see fig. 1(b) and (c). Because the adjacency matrix is symmetric with $A_{ji} = A_{ij}$, the "necklace" contains a central cluster with degree $k_{\rm ce}$. The remaining rectangular clusters correspond to bilayers, in which vertices of low degree $k < k_{\rm ce}$ on one side are connected to vertices with high degree $k > k_{\rm ce}$ on the other side. In each bilayer, all low-degree vertices have the same degree k, while the high-degree vertices cover a whole range of k-values. We denote the two boundary values of this range by κ_n and κ_{n-1}, such that a bilayer consists of vertices with low-degree k_n and vertices with high-degrees $\kappa_n < k < \kappa_{n-1}$. Furhermore, we define $\kappa_{-1} \equiv k_{\rm max}$, so that the outermost bilayer consists of the k_0-vertices that are connected to the high-degree vertices with $\kappa_0 < k < k_{\rm max}$. The next bilayer consists of all vertices with degree k_1 and all vertices with $\kappa_1 < k < \kappa_0$ and so forth. Note that $\kappa_{n-1} > \kappa_n$, since the enumeration starts from the outermost bilayer. The k_n-cluster then contains all edges between the low-degree k_n-vertices and the high-degree κ_n-band corresponding to a rectangular region in fig. 1(b) and (c). The k_n-cluster of edges together with the k_n-vertices and the vertices of the κ_n-band form a bipartite subgraph of the network. Further inspection of fig. 1(b) and (c) also shows that the number of edges that i) emanate from the k_n-vertices or from the κ_n-band and ii) do *not* belong to the k_n-cluster is relatively small. In this way, the k_n-vertices and the κ_n-band form a bilayer in k-space with many interior and relatively few exterior connections.

The values of the boundary degrees κ_n can be obtained iteratively from a bipartite approximation, in which we ignore the exterior connections between the bilayers. Thus, assume that all edges emanating from the k_0-vertices provide connections to the κ_0-band with $\kappa_0 \leqslant k \leqslant k_{\rm max}$ and vice versa. This assumption leads to the implicit equation $P(k_0)\, k_0 = \sum_{k=\kappa_0}^{k_{\rm max}} P(k)\, k$ for κ_0. Likewise, the value of κ_1 then follows from $P(k_1)\, k_1 = \sum_{k=\kappa_1}^{\kappa_0} P(k)\, k$, etc.

Using the degree distribution $P(k)$ as in (1) and approximating the sums by integrals, the boundary degrees κ_n can be calculated explicitly. The boundary degree κ_0, *e.g.*, is found to behave as

$$\kappa_0 \approx \kappa_0^\infty \equiv k_0^{(\gamma-1)/(\gamma-2)} (\gamma-2)^{1/(2-\gamma)} \tag{3}$$

for large N. The N-independent value of κ_0^∞ agrees very well with the numerical results in fig. 1(a).

The bipartite approximation just described ignores the exterior connections between the bilayers. In general, these latter connections play an important role as well since they ensure that the networks are fully connected and cannot be decomposed into disjoint subgraphs.

For large N, the central degree $k_{\rm ce}$ can be estimated by the boundary degree $\kappa_{\rm ce}$ as obtained from the implicit equation

$$\int_{k_0}^{\kappa_{\rm ce}} {\rm d}k\, P(k)\, k = \int_{\kappa_{\rm ce}}^{k_{\rm max}} {\rm d}k\, P(k)\, k, \tag{4}$$

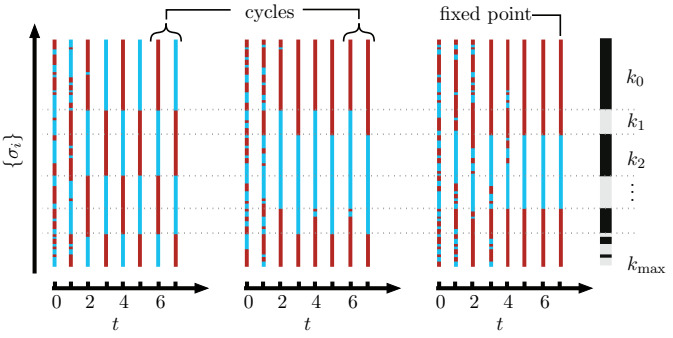

Fig. 2: Evolution of three spin patterns $\{\sigma_i\}$ with time t on a small network with $N = 64$, $\gamma = 2.9$ and $k_0 = 6$. Each column contains all the vertices of the network, The vertices are ordered according to their degree, starting from the k_0-vertices at the top to the $k_{\rm max}$-vertex at the bottom, see bar on the right. Spin-up and spin-down states are shown in red and blue, respectively.

which represents the condition that the vertices with degrees $k < \kappa_{\rm ce}$ are connected to the same number of edges as the vertices with degrees $k > \kappa_{\rm ce}$.

Using the scale-free degree distribution (1) in (4), the central degree $k_{\rm ce}$ is found to behave as

$$k_{\rm ce} \approx \kappa_{\rm ce} = 2^{\frac{1}{\gamma-2}} k_0 (1 + N^{\frac{2-\gamma}{\gamma-1}})^{\frac{1}{2-\gamma}} \leqslant 2^{\frac{1}{\gamma-2}} k_0 \tag{5}$$

for large N. Therefore, the number $N_{\rm bi}$ of bilayers behaves as

$$N_{\rm bi} = k_{\rm ce} - k_0 \approx (2^{\frac{1}{\gamma-2}} - 1) k_0 \quad \text{for large} \quad N. \tag{6}$$

This number diverges as γ approaches two from above.

Majority rule dynamics. – Now, we place binary variables or spins $\sigma_i = \pm 1$ on each vertex i. The pattern $\{\sigma_i(t)\}$ of all spins is taken to evolve according to the majority rule

$$\sigma_i(t+1) = {\rm sgn}\left[\sum_{j=1}^{N} A_{ij}\sigma_j(t)\right]; \tag{7}$$

in the special case $\sum_{j=1}^{N} A_{ij}\sigma_j(t) = 0$, we choose $\sigma_i(t+1) = \pm 1$ with equal probability. All σ_i are updated simultaneously. For uncorrelated scale-free networks, the majority rule dynamics exhibits only two attractors corresponding to patterns with all spins pointing either up or down [15,16]. When we rewire these networks to obtain dissortative mixing, we find a completely different behavior. Figure 2 illustrates the time evolution of three random initial patterns on a small, maximally dissortative network. First, we observe that the three initial patterns do not evolve towards one of the two completely ordered states, but that additional attractors emerge, in our example two cycles and one fixed point. Indeed, we find that attractors consist, in general, of two alternating patterns denoted by $\{\Sigma\}$ and $\{\Sigma^*\}$. A global fixed point represents a special case with $\{\Sigma^*\} = \{\Sigma\}$.

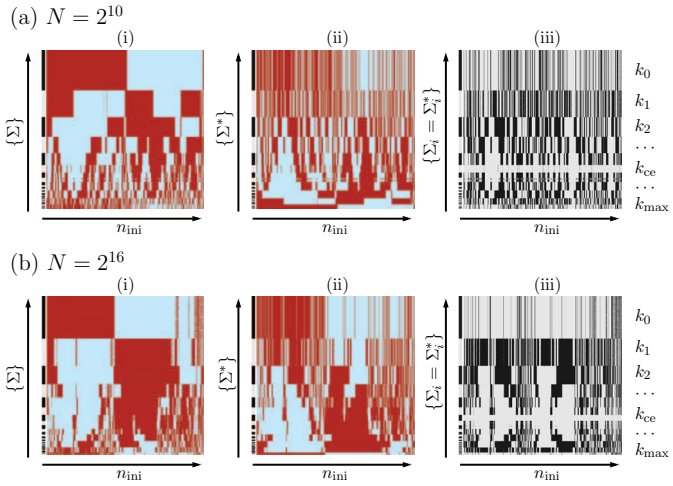

Fig. 3: Visualization of attractors as obtained from $n_{\rm ini} = 1000$ initial patterns for two networks with $\gamma = 2.9$, $k_0 = 6$ and different sizes (a) $N = 2^{10}$ and (b) $N = 2^{16}$. All attractors consist of two alternating spin patterns $\{\Sigma\}$ and $\{\Sigma^*\}$, which are shown in panels (i) and (ii). Each column represents the states of all N vertices, which are ordered by degree as in fig. 2. The x-axis corresponds to different initial configurations. For clarity, the different attractors are ordered by their Hamming-distance to the all-spin-up pattern. Panels (iii) combine the two attractor states in (i) and (ii): vertices within bilayer fixed points and bilayer blinkers are shown in light grey and black, respectively.

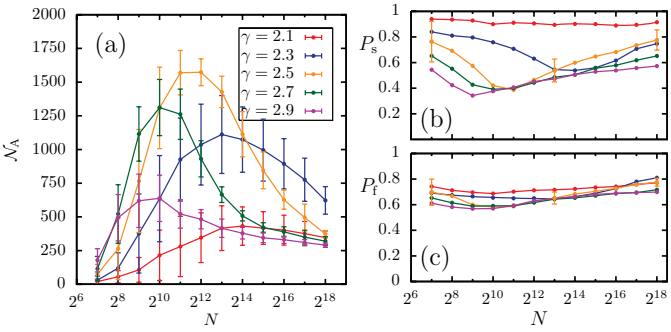

Fig. 4: (a) Number of attractors $\mathcal{N}_{\rm A}$ as a function of network size N. (b) Probability $P_{\rm s}$ that neighboring layers of k and $k+1$ vertices are in the same state as a function N. (c) Probability $P_{\rm f}$ that any k-layer with $k_0 \leqslant k \leqslant k_{\rm ce}$ belongs to a bilayer fixed point as a function of N. All data were obtained from 2000 simulated random initial configurations and are averaged over 100 networks with the same values for N, γ and $k_0 = 6$. Error bars correspond to the standard deviation.

Second, all attractors can be characterized by the behavior of the bilayers as introduced above. Indeed, all k_n-vertices attain the same spin value as do all vertices within the κ_n-band. The corresponding subset of spins will be denoted by $\{\Sigma\}_n$. For each bilayer, the k_n-vertices can exhibit two types of dynamical behavior: i) the spins of all k_n-vertices remain unchanged with $\{\Sigma^*\}_n = \{\Sigma\}_n$, which implies a bilayer fixed point, for which the spins of the κ_n-band have the same value as those of the k_n-vertices; and ii) the spin pattern of the k_n-vertices alternates at every time step with $\{\Sigma^*\}_n = -\{\Sigma\}_n$ corresponding to a blinking bilayer, for which the spins of the κ_n-band have opposite values to those of the k_n-vertices.

Dependence of attractor number on network size. – In order to determine the total number of attractors, we have performed extensive computer simulations starting from a large number of different initial patterns. It is hardly possible to explore all 2^N initial patterns, even for moderate N. In our simulations, we therefore restrict ourselves to strongly disordered initial configurations, for which i) $\langle \sigma(t=0) \rangle = 0$ and ii) a randomly chosen neighbor of any vertex in the network is in the spin-up or -down state with equal probability. For each network with a given set of parameters (N, γ, k_0), we simulate $n_{\rm ini} = 2000$ initial states and average the resulting number of different attractors over an ensemble of 100 networks with identical parameters. Figure 3 illustrates the attractors obtained for $n_{\rm ini} = 1000$ random initial configurations on two networks that differ only in their size. Each bilayer can attain a bilayer fixed point or a bilayer blinker, but different bilayers can act independently from each other. The $k_{\rm ce}$-vertices of the central cluster always attain the same, fixed spin value. Although the absolute network sizes in fig. 3(a) and (b) differ by a factor of 64, the number of bilayers is the same for both network sizes, and we therefore observe very similar overall attractor states.

If we again ignored the exterior connections between the bilayers, each possible attractor would consist of a central cluster, for which all spins point either up or down, and $N_{\rm bi}$ bilayer fixed points or bilayer blinkers. The maximal number of such attractors is given by

$$\max(\mathcal{N}_{\rm A}) = 4^{N_{\rm bi}} + 2^{N_{\rm bi}} \leqslant 4^{\zeta k_0} + 2^{\zeta k_0} \qquad (8)$$

with $\zeta \equiv (2^{\frac{1}{\gamma-2}} - 1)$ as follows from (6). We would therefore expect that the number $\mathcal{N}_{\rm A}$ of attractors first grows with network size N and then saturates for sufficiently large N.

Surprisingly, the N-dependence of $\mathcal{N}_{\rm A}$ is more complicated: As shown in fig. 4(a), the attractor number $\mathcal{N}_{\rm A}$ is a *nonmonotonic* function of N with a maximum at intermediate N-values. For (N, γ, k_0)-values for which $\mathcal{N}_{\rm A}$ is comparatively large, its precise value cannot be determined via numerical simulations, since an increase in the number of initial configurations will also increase the number of observed attractors. To ensure that the observed maximum is not an artifact arising from computational limitations, we carefully examined the scaling of $\mathcal{N}_{\rm A}$ as a function of the number of initial configurations $n_{\rm ini}$. Figure 5(a) shows the number of attractors as a function of $n_{\rm ini}$ for three particular networks with $\gamma = 2.9$, $k_0 = 6$ and different sizes $N = 2^7$, $N = 2^{10}$ and $N = 2^{16}$. In total, 2^{15} initial configurations were simulated for each network and for $n_{\rm ini} = 2^1, 2^2, 2^3, \ldots, 2^{15}$ the

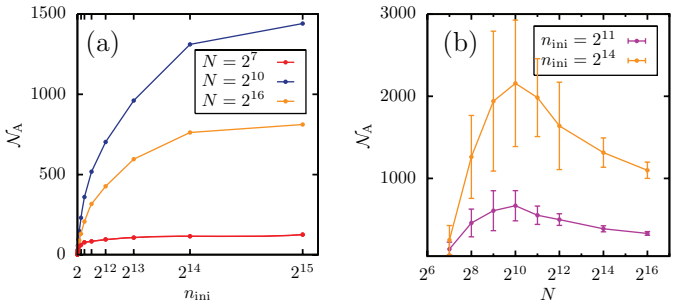

Fig. 5: (a) Number of attractors $\mathcal{N}_A$ as a function of the number n_{ini} of simulated initial configurations for three particular networks with $\gamma = 2.9$, $k_0 = 6$ and different network sizes $N = 2^7$, $N = 2^{10}$ and $N = 2^{16}$. (b) $\mathcal{N}_A$ as a function of N for $n_{ini} = 2^{11}$ and $n_{ini} = 2^{14}$. All networks have $\gamma = 2.9$ and $k_0 = 6$. One data point was obtained by averaging over 50 different networks with the same values for N, γ and k_0, error bars show the standard deviation around the mean.

respective number of different attractors was counted. We see that for $n_{ini} \gtrsim 2^{14}$, the number of attractors saturates: As n_{ini} is increased by a factor 2, only a few additional attractors are found. Figure 5(b) displays the dependence of the number of attractors on the network size for two different values of n_{ini}. The magenta curve has the same parameters, $\gamma = 2.9$, $k_0 = 6$ and $n_{ini} = 2^{11}$, as the corresponding magenta curve in fig. 4(a). The yellow curve shows the results for $n_{ini} = 2^{14}$, so eight times as many initial configurations were simulated compared to the magenta curve. We see that the maximum at intermediate network sizes becomes even more pronounced, while the qualitative behavior of $\mathcal{N}_A(N)$ remains unchanged.

Evolution of attractor ensembles. – A closer inspection of the panels iii) in fig. 3(a) and (b) reveals two main differences in the ensemble of attractors for the two network sizes. First, the inner bilayers close to the central cluster tend to be more synchronized for the larger network. Second, we note an increasing amount of bright areas, indicating more bilayer fixed points for larger N. In order to elucidate these two tendencies, we measured the probability $P_s \equiv \langle P(\{\Sigma\}_{k+1} = \{\Sigma\}_k)\rangle$ that neighboring layers of k and $k+1$ vertices are in the same state as well as the probability $P_f \equiv \langle P(\{\Sigma^*\}_k = \{\Sigma\}_k)\rangle$ that any k-layer belongs to a bilayer fixed point. Both probabilities were computed and averaged over all k-values with $k_0 \leqslant k \leqslant k_{ce}$.

As shown in fig. 4(b), small networks are characterized by a large value of the probability P_s, which is understandable since the k_{max}-vertex is very dominant for small N and interconnects several low degree layers, see (2). With increasing N, the number of these layers becomes smaller and the probability P_s decreases, see fig. 4(b). However, after a minimum at intermediate network sizes, P_s starts to increase again. The same behavior is found for the probability P_f in fig. 4(c). Once the number N_{bi} of bilayers has reached its maximal number, bilayer blinkers become less likely with increasing N. For each value of γ, the two N-values, at which the probabilies P_s and P_f reach their minima in fig. 4(b) and (c), agree quite well with the N-value for the maximum in fig. 4(a).

Summary and outlook. – In summary, we showed that dissortative scale-free networks as frequently found in nature are characterized by a nested bilayer structure. This structure strongly affects dynamical processes on these networks as shown explicitly for majority rule dynamics. The number of attractors reaches a maximum at intermediate, "optimal" network sizes.

To test the robustness of our results, we examined several variations on the structural details of the system. By explicit simulations, we verified that the nonmonotonic behavior in the number of attractors is also found for majority dynamics on directed networks, for which the in- and out-degree, k_{in} and k_{out}, are identical at each vertex. Since many properties of scale-free networks depend sensitively on the scaling behaviour of the upper cut-off k_{max} (see, *e.g.*, [24–26]), we also considered networks with the so-called structural cut-off $k_{max} = k_0\sqrt{N}$, as introduced in [24]. Again, we find a nested bilayer structure and a maximum in the number of attractors.

Thus, our study reveals a class of dynamical processes for which the most complex behavior is found for *intermediate* rather than for large network sizes. Therefore, it should be rather interesting to elucidate the N-dependence of previously studied properties of dissortative networks, such as synchronization times [27] or response behavior [28,29].

REFERENCES

[1] Strogatz S. H., *Nature*, **410** (2001) 268.
[2] Boccaletti S., Latora V., Moreno Y., Chavez M. and Hwang D.-U., *Phys. Rep.*, **424** (2006) 175.
[3] Ciliberti S., Martin O. C. and Wagner A., *Proc. Natl. Acad. Sci. U.S.A.*, **104** (2007) 13591.
[4] Li F., Long T., Lu Y., Ouyang Q. and Tang C., *Proc. Natl. Acad. Sci. U.S.A.*, **101** (2004) 4781.
[5] Hopfield J. J., *Proc. Natl. Acad. Sci. U.S.A.*, **79** (1982) 2554.
[6] Bar-Yam Y. and Epstein I. R., *Proc. Natl. Acad. Sci. U.S.A.*, **101** (2004) 4341.
[7] Newman M. E. J., *SIAM Rev.*, **45** (2003) 167.
[8] Albert R. and Barabási A.-L., *Rev. Mod. Phys.*, **74** (2002) 47.
[9] Newman M. E. J., *Phys. Rev. Lett.*, **89** (2002) 208701.
[10] Newman M. E. J., *Phys. Rev. E*, **67** (2003) 026126.
[11] Glauber R. J., *J. Math. Phys.*, **4** (1963) 294.
[12] Li P. P., Zheng D. F. and Hui P. M., *Phys. Rev. E*, **73** (2006) 056128.
[13] Spirin V., Krapivsky P. and Redner S., *Phys. Rev. E*, **63** (2001) 36118.
[14] Spirin V., Krapivsky P. and Redner S., *Phys. Rev. E*, **65** (2001) 16119.
[15] Zhou H. and Lipowsky R., *Proc. Natl. Acad. Sci. U.S.A.*, **102** (2005) 10052.

[16] Zhou H. and Lipowsky R.,2007 *J. Stat. Mech.* (2007) P01009.
[17] Krapivsky P. L. and Redner S., *Phys. Rev. Lett.*, **90** (2003) 238701.
[18] Lambiotte R., *J. Phys. A*, **41** (2008) 224021.
[19] Cohen R., Erez K., Ben-Avraham D. and Havlin S., *Phys. Rev. Lett.*, **85** (2000) 4626.
[20] Maslov S. and Sneppen K., *Science*, **296** (2002) 910.
[21] Pastor-Satorras R., Vázquez A. and Vespignani A., *Phys. Rev. Lett.*, **87** (2001) 258701.
[22] Molloy M. and Reed B., *Random Struct. & Alg.*, **6** (1995) 161.
[23] Xulvi-Brunet R. and Sokolov I. M., *Phys. Rev. E*, **70** (2004) 066102.
[24] Boguñá M., Pastor-Satorras R. and Vespignani A., *Eur. Phys. J. B*, **38** (2004) 205.
[25] Catanzaro M., Boguñá M. and Pastor-Satorras R., *Phys. Rev. E*, **71** (2005) 027103.
[26] Weber S. and Porto M., *Phys. Rev. E*, **76** (2007) 46111.
[27] Sorrentino F., Dibernardo M., Cuellar G. and Boccaletti S., *Physica D*, **224** (2006) 123.
[28] Wang S. J., Wu A. C., Wu Z. X., Xu X. J. and Wang Y. H., *Phys. Rev. E*, **75** (2007) 046113.
[29] Brede M. and Sinha S., arXiv e-prints, cond-mat/0507710v1 (2005).